Cellular/Molecular

Kinase-Dead Knock-In Mouse Reveals an Essential Role of Kinase Activity of Ca^{2+}/Calmodulin-Dependent Protein Kinase IIα in Dendritic Spine Enlargement, Long-Term Potentiation, and Learning

Yoko Yamagata,[1,2,3] Shizuka Kobayashi,[4] Tatsuya Umeda,[5] Akihiro Inoue,[5] Hiroyuki Sakagami,[6] Masahiro Fukaya,[7] Masahiko Watanabe,[7] Nobuhiko Hatanaka,[8] Masako Totsuka,[3] Takeshi Yagi,[10] Kunihiko Obata,[9] Keiji Imoto,[1,2] Yuchio Yanagawa,[3,11] Toshiya Manabe,[3,4] and Shigeo Okabe[12]

[1]Department of Information Physiology, National Institute for Physiological Sciences, and [2]The Graduate University for Advanced Studies (SOKENDAI), Okazaki 444-8787, Japan, [3]Core Research for Evolutional Science and Technology, Japan Science and Technology Agency, Kawaguchi 332-0012, Japan, [4]Division of Neuronal Network, Institute of Medical Science, University of Tokyo, Tokyo 108-8639, Japan, [5]Department of Cell Biology, Tokyo Medical and Dental University, Tokyo 113-8519, Japan, [6]Department of Anatomy, Kitasato University School of Medicine, Sagamihara 228-8555, Japan, [7]Department of Anatomy, Hokkaido University School of Medicine, Sapporo 060-8638, Japan, [8]Division of System Neurophysiology and [9]Laboratory of Neurochemistry, National Institute for Physiological Sciences, Okazaki 444-8585, Japan, [10]Graduate School of Frontier Biosciences, Osaka University, Suita 565-0871, Japan, [11]Department of Genetic and Behavioral Neuroscience, Gunma University Graduate School of Medicine, Maebashi 371-8511, Japan, and [12]Department of Cellular Neurobiology, Graduate School of Medicine, University of Tokyo, Tokyo 113-0033, Japan

Ca^{2+}/calmodulin-dependent protein kinase IIα (CaMKIIα) is an essential mediator of activity-dependent synaptic plasticity that possesses multiple protein functions. So far, the autophosphorylation site-mutant mice targeted at T286 and at T305/306 have demonstrated the importance of the autonomous activity and Ca^{2+}/calmodulin-binding capacity of CaMKIIα, respectively, in the induction of long-term potentiation (LTP) and hippocampus-dependent learning. However, kinase activity of CaMKIIα, the most essential enzymatic function, has not been genetically dissected yet. Here, we generated a novel CaMKIIα knock-in mouse that completely lacks its kinase activity by introducing K42R mutation and examined the effects on hippocampal synaptic plasticity and behavioral learning. In homozygous CaMKIIα (K42R) mice, kinase activity was reduced to the same level as in CaMKIIα-null mice, whereas CaMKII protein expression was well preserved. Tetanic stimulation failed to induce not only LTP but also sustained dendritic spine enlargement, a structural basis for LTP, at the Schaffer collateral–CA1 synapse, whereas activity-dependent postsynaptic translocation of CaMKIIα was preserved. In addition, CaMKIIα (K42R) mice showed a severe impairment in inhibitory avoidance learning, a form of memory that is dependent on the hippocampus. These results demonstrate that kinase activity of CaMKIIα is a common critical gate controlling structural, functional, and behavioral expression of synaptic memory.

Introduction

Activity-dependent synaptic plasticity in the hippocampus, as represented by long-term potentiation (LTP) in the CA1 region, is considered to be one of the fundamental mechanisms for learning and memory (Bliss and Collingridge, 1993; Malenka and Bear, 2004). Extensive studies in search for molecular basis for LTP identified Ca^{2+}/calmodulin-dependent protein kinase II (CaMKII) as a leading candidate involved in such a process (Hudmon and Schulman, 2002; Lisman et al., 2002; Colbran and Brown, 2004). CaMKII exists abundantly in the CNS and is a major constituent of the postsynaptic density (PSD). CaMKII is composed of structurally related, homologous isoforms (subunits) derived from four distinct genes (i.e., CaMKIIα, CaMKIIβ, CaMKIIγ, and CaMKIIδ). Among them, CaMKIIα and CaMKIIβ are predominant in the brain and show neuron-specific expression, but their regional distributions are distinct, with CaMKIIα dominant in the forebrain, and with CaMKIIβ dominant in the cerebellum. CaMKIIα is especially enriched in the hippocampus, and therefore it seems to be the indispensable isoform that is involved in hippocampal synaptic plasticity. The neuronal CaMKII holoenzyme is a multimeric complex assembled from 12 subunits consisting of CaMKIIα and/or CaMKIIβ, depending on their abundance in specific brain regions.

Received Feb. 11, 2009; revised April 23, 2009; accepted April 30, 2009.

This work was supported by Grants-in-Aid for Scientific Research from Japan Society for the Promotion of Science (KAKENHI) (Yo.Y., K.O., K.I., Yu.Y., T.M., S.O.), Brain Science Foundation (Yu.Y.), Center for Brain Medical Science, 21st Century Center of Excellence Program (T.M.), and The Novartis Foundation (Japan) for the Promotion of Science (T.M.). We thank T. Yamauchi for rat CaMKIIα cDNA, H. Fujisawa and S. Okuno for a CaMKIIα antibody for initial experiments, Y. Fukazawa for perfusion, R. Ijuin, Y. Mashiko, and N. Kume for technical assistance, S. Kida for advice on behavioral experiments, and F. Murakami and Y. Kubo for critical reading of the initial version of this manuscript. We also thank staffs in the Center for Experimental Animals at the National Institute for Physiological Sciences.

Correspondence should be addressed to Dr. Yoko Yamagata, Department of Information Physiology, National Institute for Physiological Sciences, Myodaiji, Okazaki 444-8787, Japan. E-mail: yamagata@nips.ac.jp.

DOI:10.1523/JNEUROSCI.0707-09.2009

 0270-6474/09/297607-12$15.00/0

According to the current hypothesis, strong synaptic activation induces LTP by way of postsynaptic Ca^{2+} influx through NMDA-type glutamate receptors (NMDARs) (Bliss and Collingridge, 1993; Malenka and Bear, 2004). Ca^{2+} influx causes activation of CaMKII by binding of Ca^{2+}/calmodulin and the following translocation of CaMKII to postsynaptic sites, whereby it binds to postsynaptic proteins, such as NMDARs (Hudmon and Schulman, 2002; Lisman et al., 2002; Colbran and Brown, 2004). Activated CaMKII undergoes T286 autophosphorylation through an intersubunit mechanism, which endows the kinase with the Ca^{2+}/calmodulin-independent autonomous activity and prolongs its association to postsynaptic sites. Such persistently activated CaMKII phosphorylates AMPA-type glutamate receptors (AMPARs) and/or AMPAR-associated proteins, leading to a prolonged enhancement of AMPAR-mediated synaptic transmission (i.e., LTP) (Derkach et al., 1999; Hayashi et al., 2000; Tomita et al., 2005). The importance of binding of Ca^{2+}/calmodulin and the following postsynaptic translocation, and the autonomous activity of CaMKIIα was supported by the previously reported CaMKIIα (T305D) and CaMKIIα (T286A) knock-in mice, respectively, because both of them showed an impairment in LTP and learning (Giese et al., 1998; Elgersma et al., 2002).

On the other hand, recent high-resolution microscopic examinations indicated that LTP is associated with long-lasting enlargement of dendritic spines (Matsuzaki et al., 2004; Okamoto et al., 2004; Otmakhov et al., 2004; Harvey and Svoboda, 2007; Zhang et al., 2008), and here again, the involvement of CaMKII has been implicated (Matsuzaki et al., 2004; Otmakhov et al., 2004; Honkura et al., 2008; Zhang et al., 2008). However, studies using previously reported CaMKIIα knock-in mice have not yet explored LTP-associated spine structural plasticity, and critical evidence for the involvement of kinase activity of CaMKIIα in prolonged spine enlargement is still lacking.

In this study, we generated a novel CaMKIIα (K42R) knock-in mouse to explore the role of kinase activity of CaMKIIα in spine structural plasticity, LTP, and learning.

Materials and Methods

Generation of the CaMKIIα (K42R) knock-in mouse. CaMKIIα gene fragments were cloned from a TT2 (F_1 hybrid between C57BL/6 and CBA) genomic library (Yagi et al., 1993) by using a *Sma*I-digested 5′-terminal 0.45 kbp fragment of rat CaMKIIα cDNA (Yamauchi et al., 1989) that encodes part of the catalytic domain, as a probe. Based on a previously reported rat CaMKIIα genomic structure (Nishioka et al., 1996), a 7.9 kbp *Kpn*I/*Xba*I fragment that encodes exon 2 containing Lys-42 (AAG) was subcloned into pBluescript (Stratagene). K42R mutation was introduced by replacing the 136 bp *Sma*I/*Hin*dIII fragment with an oligonucleotide encoding the mutation (Arg-42, A**G**G), as indicated in Figure 1*A*. This mutation simultaneously generated a new *Bst*NI site to facilitate its detection. A PGK-neo cassette [PGK-Neo-poly(A)], a G418-selectable marker, flanked by two loxP sites was inserted in the *Apa*I site 790 bp downstream of the targeted exon 2. A diphtheria toxin A cassette [MC1-DT-A-poly(A)] was included in the targeting vector to allow selection against random integration (Yanagawa et al., 1999). The linearized targeting vector was electroporated into TT2 ES cells. Homologous recombination was detected in G418-resistant colonies by PCR using combinations of the following oligonucleotide primers: 5′-terminal sense 4.4 kbp upstream of exon 2, locating outside the targeting vector (5′-TGTGCTCTTGACTGAGATCCTCCCTC-3′); 5′-terminal antisense within the PGK-neo cassette (5′-AAAGCGCATGCTCCAGACTGCCTTG-3′); 3′-terminal sense within the PGK-neo cassette (5′-TGAAGAACGAGATCAGCAGCCTCTGT-3′); and 3′-terminal antisense 3.5 kbp downstream of exon 2, locating outside the targeting vector (5′-GCTCCTCAGACAGATCCAAGCTCAAG-3′). Four of 524 colonies showed the PCR products of expected size, and homologous recombination was further verified by Southern blot analyses. The PGK-neo cassette was then removed by transient expression of Cre recombinase (pCre-Pac) (Taniguchi et al., 1998). The final positive ES cells were injected into eight cell embryos from ICR mice to obtain chimeras (Yagi et al., 1993). Heterozygous mice were obtained by crossing the chimeric mice with C57BL/6 or ICR female mice. Homozygous K42R and control wild-type mice were obtained by crossing heterozygous mice.

Homologous recombination was confirmed by Southern blot analyses of mouse genomic DNA using a 3′ external probe (i.e., a 0.23 kbp *Xba*I–*Hin*dIII genomic fragment just downstream of the targeting site) and an internal probe (i.e., a 1.1 kbp *Apa*I–*Apa*I genomic fragment that contains exon 2) (see Fig. 1*A*). Mouse genomic DNA was digested by *Apa*I for the 3′ probe and by *Eco*RV for the internal probe, respectively (see Fig. 1*B*). Genotypes of mice were determined by PCR using oligonucleotide primers 5′-sense (5′-GGTCTTGAAGACTGTCTGGTGTGAGA-3′) and 3′-antisense (5′-CACAGGCCAGTTTAGGTCTTGCTAGG-3′) to amplify the loxP insertion site (see Fig. 1*C*). Another PCR was performed using oligonucleotide primers 5′-sense (5′-CAGCTCCCTTCCTTGCATGGTACATC-3′) and 3′-antisense (5′-AGGGGTCAAGTTTGGGGTTCAGGTCT-3′) to amplify the region containing exon 2, and the PCR products were digested by *Bst*NI to detect a new restriction site generated by the mutation (see Fig. 1*D*). Alternatively, the PCR products were purified and subjected to direct nucleotide sequencing to detect the nucleotide replacement (see Fig. 1*E*).

Animal experiments. Animal experiments were reviewed and approved by the Animal Care and Use Committees of the Okazaki Organization of National Institutes of Natural Sciences and affiliated universities. All experiments were conducted in accordance with the Guide for Animal Experimentation in corresponding institutes and universities. Animals were housed in cages with *ad libitum* access to water and food and maintained on a 12 h light/dark cycle.

All analyses were performed using adult male or female homozygous or heterozygous CaMKIIα (K42R) and wild-type littermate mice generated by intercrosses between heterozygous mice unless otherwise specified. Rating of survival, *in situ* hybridization, and biochemical experiments were performed in mice backcrossed to C57BL/6 for one generation. Immunoelectron microscopic analysis, electrophysiological experiments, and behavioral analyses were performed in mice backcrossed to C57BL/6 for more than six generations. Culture studies were performed in mice backcrossed to ICR for two or three generations.

CaMKIIα knock-out mice were purchased from The Jackson Laboratory. Since there were breeding difficulties in female heterozygous knock-out mice (Hinds et al., 1998), male heterozygous mice were crossed with female wild-type C57BL/6 mice, and resultant heterozygous knock-out and wild-type offspring were analyzed.

Sample preparation for biochemical analyses. Forebrain and cerebellar homogenates were prepared as previously described (Yamagata et al., 2006). Animals were decapitated under pentobarbital (50 mg/kg) or carbon dioxide anesthesia. Brains were removed quickly, put in ice-cold homogenization buffer within 30 s after decapitation, and left in the buffer for 30 s for chilling. Forebrain (without diencephalon and striatum) and cerebellum were dissected on an ice-cold Petri dish and immediately homogenized in a fivefold volume of homogenization buffer in a Teflon-glass homogenizer on ice. The homogenization buffer consisted of 20 mM Tris/HCl, pH 7.5, 5 mM EDTA, 1 mM EGTA, 10 mM sodium pyrophosphate, 50 mM NaF, 1 mM Na_3VO_4 (ortho), 1 mM dithiothreitol, 10 μg/ml each of leupeptin, antipain, pepstatin, and chymostatin, 0.1 mM phenylmethylsulfonyl fluoride, and 0.1 μM calyculin A. Each sample was quickly aliquoted, an aliquot was saved for the preparation of samples for SDS-PAGE, another for the measurement of protein concentration, and the rest were frozen immediately and stored at −80°C until additional characterization of kinase activity. Protein concentration was determined by using BCA Protein Assay Reagent (Pierce) and bovine serum albumin as a standard.

CaMKII kinase activity assay. CaMKII kinase activity assay was performed as previously described (Yamagata et al., 2006) with some modifications. The assay was conducted in the presence of 50 mM HEPES/NaOH, pH 7.5, 10 mM magnesium acetate, 1 mM EGTA, 50 μg/ml BSA,

0.1% Triton X-100, 50 μM autocamtide-2 [KKALRRQETVDAL (Hanson et al., 1989); synthesized by Mimotopes], 2 μM PKI-(5–24)-amide (Peninsula Laboratories), 2 μM PKC-(19–36)-amide (Peninsula Laboratories), 100 μM [γ-^{32}P]ATP (400–800 cpm/pmol; PerkinElmer Life and Analytical Sciences), and with (for the total activity) or without (for the Ca^{2+}/calmodulin-independent autonomous activity) 1.5 mM $CaCl_2$ and 25 μg/ml calmodulin in a final volume of 50 μl. The reaction was started by the addition of [γ-^{32}P]ATP, performed for 1 min at 30°C, and terminated by the addition of acetic acid (final concentration, 10%). After spotting aliquots onto pieces of P81 phosphocellulose papers (Whatman) and washing the papers with 75 mM phosphoric acid, the retained radioactivity on the papers was measured in a beta scintillation counter (Beckman Coulter). The amount of protein used for the kinase activity assay was 0.6 and 1.0 μg from forebrain and cerebellar homogenates, respectively, and the reaction was linear in terms of both protein concentration and incubation time.

Immunoblot analyses. Quantitative immunoblot analyses were performed as described previously (Yamagata et al., 2006). Antibodies against CaMKIIα (mouse monoclonal; 6G9; 1:1000; BIOMOL), CaMKIIβ (mouse monoclonal; CBb-1; 1:200; Zymed), CaMKIIγ (goat polyclonal; C-18; 1:200; Santa Cruz Biotechnology), CaMKIIδ (rabbit polyclonal; 1:125; Transgenic), and phospho-T286-CaMKIIα (rabbit polyclonal; 1:500; Promega) were used for the primary reaction. For mouse and goat antibodies, rabbit anti-mouse and anti-goat IgG (1:500; MP Biomedicals) were used in the secondary reaction, respectively. Blots were then visualized by using ^{125}I-protein A ($3.5–5 \times 10^5$ cpm/ml; PerkinElmer Life and Analytical Sciences), and the radioactivity was measured in a gamma counter (Aloka). The amounts of protein used were as follows: forebrain homogenate, 2 μg (anti-CaMKIIα, anti-CaMKIIγ, and anti-CaMKIIδ), 4 μg (anti-CaMKIIβ), and 8 μg (anti-phospho-T286-CaMKIIα); cerebellar homogenate, 2 μg (anti-CaMKIIγ and anti-CaMKIIδ), 4 μg (anti-CaMKIIβ), 8 μg (anti-CaMKIIα), and 32 μg (anti-phospho-T286-CaMKIIα). The measured immunoreactivity was in a linear range in terms of protein amounts used for each antibody. The values obtained from mutant samples were expressed as percentages against those from control wild-type samples on the same blots.

In situ *hybridization. In situ* hybridization histochemistry with radioactive oligonucleotides was performed as described previously (Sakagami et al., 2004). The oligonucleotide probes specific for individual isoforms of CaMKII were as follows: CaMKIIα, 5′-CCAAAGGAGAACCAGCAGCCACATTCCACGGACAAAGAGCGGATC-3′; CaMKIIβ, 5′-GGAGCAGCAGCAACTCTCAGGCACAACTAGCAGGAAAGGAGGCAG-3′; CaMKIIγ, 5′-GCCCACTGTTCATGCCTGGATGAGCATCACACAAACTCCTGTCTC-3′; CaMKIIδ, 5′-GCTAGCTAGTGAAAGTGAGGCAGGAAATGTCCTCTGACCCAGGTTG-3′.

Immunoelectron microscopic analysis. Postembedding immunogold analysis was performed as reported previously (Fukaya and Watanabe, 2000). Ultrathin sections on nickel grids were treated successively with 1% human serum albumin (Wako)/0.1% Tween 20 in TBS (HTBST), pH 7.5, for 1 h, mouse anti-CaMKIIα (6G9; Millipore Bioscience Research Reagents) or rabbit anti-PSD-95 antibodies (Fukaya and Watanabe, 2000) (15 μg/ml for each) in HTBST overnight, and colloidal gold (10 nm)-conjugated anti-mouse or rabbit IgG (1:100; British Bio Cell International) in HTBST for 2 h. Finally, grids were stained with uranyl acetate for 15 min and examined with an H-7100 electron microscope (Hitachi). For quantitative analysis, immunogold particles on the PSD of axospinous asymmetrical synapses were counted on electron micrographs.

Generation of recombinant adenoviruses. The generation and characterization of recombinant adenoviruses expressing enhanced green fluorescent protein (EGFP)-Homer1c were described previously (Okabe et al., 2001). Expression plasmids for wild-type and K42R-mutant CaMKIIα N-terminally labeled with EGFP were generated by inserting respective full-length cDNAs into pEGFP-C1 (Clontech). K42R-mutant CaMKIIα was generated from wild-type CaMKIIα using PCR and the QuickChange Site-Directed Mutagenesis kit (Stratagene). Replication-deficient adenoviruses were prepared as described previously (Okabe et al., 1999).

Hippocampal neuronal culture. Cell suspensions were prepared individually from every embryo at the age of embryonic day 16.5 of gestation from female heterozygous mice mated with male heterozygous mice. The extremities of each embryo were saved for genotyping. The hippocampus was dissected in Ca^{2+}, Mg^{2+}-free HBSS, free from the choroid plexus and meningeal tissue. The two hippocampi from the same embryo were placed in a tube containing Minimum Essential Medium (MEM) with B27 supplement and 5% FCS, and then triturated by passing them several times through a P-1000 pipette. The cell suspension was plated onto glass coverslips coated with poly-L-lysine. Cells were incubated at 37°C under 5% CO_2. Two days after plating, 10 μM ara-C was added to prevent glial cell proliferation. Neurons were exposed to adenoviruses at a multiplicity of infection of 20–50 at 12–16 d after plating and maintained for 2 d before imaging.

Imaging of dissociated hippocampal neurons. Live hippocampal neurons were mounted in a chamber at 37°C with a continuous flow of humidified 5% CO_2 to maintain the pH of the medium for long time-lapse experiments. Alternatively, culture medium was replaced with Tyrode's solution (in mM: 119 NaCl, 2.5 KCl, 2 $CaCl_2$, 2 $MgCl_2$, 25 HEPES, pH 7.4, and 30 glucose) and live cells were mounted in a chamber at 37°C without a continuous gas flow. Images were obtained on a Fluoview confocal laser-scanning microscope (Olympus). A 60× oil-immersion lens (numerical aperture, 1.1) was used, and images were collected at an additional electric zoom factor from 3 to 6×. For long time-lapse imaging, multiple optical sections (*z*-spacing of 0.3–0.4 μm) were collected, and these images were recombined using a maximum-brightness operation. Fluorescence recovery after photobleaching (FRAP) experiments were performed using a Macro program to control sequential image acquisition and delivery of a photobleaching laser pulse to the region of interest defined by acousto-optic tunable filter. Uncaging of brominated 7-hydroxycoumarin-4-ylmethoxycarbonyl L-glutamate (Bhc-glu) was performed by focal illumination of dendritic segments with 405 nm diode laser beam with the duration of 100 ms. Bhc-glu was applied to the cells at the concentration of 50 μM.

Immunocytochemistry. Cells were fixed in 2% paraformaldehyde in PBS for 25 min at room temperature or with methanol for 10 min at −20°C, permeabilized by incubating with 0.2% Triton X-100 in PBS for 5 min, blocked with 5% normal goat serum, and incubated with mouse monoclonal anti-PSD-95 (Affinity Bioreagents) or rat polyclonal anti-Homer (Millipore Bioscience Research Reagents) antibodies. Primary antibodies were visualized with goat anti-mouse IgG conjugated to Cy3 (Jackson ImmunoResearch).

Hippocampal organotypic slices. Hippocampal slice cultures from postnatal day 4–5 mice were prepared as described previously (Stoppini et al., 1991). Briefly, the dissected hippocampus and cortex were cut into 375 μm slices with a McIlwain-type tissue chopper. Slices were placed on a transparent porous filter (Millicell CM; Millipore) in a 34°C, 5% CO_2 humid incubator, and fed every 3 d with culture medium containing 48% MEM, 24% Earle's balanced salt solution (EBSS), 24% heat-inactivated horse serum supplemented with 5 mg/ml glucose, 10 mM HEPES, 1 mM glutamine, penicillin, and streptomycin (50 U/ml each). The slices were used for time-lapse imaging at 12–14 d *in vitro*.

Single-cell electroporation. Pyramidal neurons were transfected with pEGFP-N1 plasmid (Clontech). Plasmid solution at the concentration of 1 ng/μl with 6 mg/ml tetramethylrhodamine (TMRD) in water was introduced into the cytoplasm of hippocampal pyramidal neurons in slice culture at 8–10 d *in vitro* by single-cell electroporation (Haas et al., 2001). Slice cultures were placed in a dish containing low serum medium (48% MEM, 43% EBSS, 5% heat-inactivated horse serum, 5 mg/ml glucose, 10 mM HEPES, and 1 mM L-glutamine) on the stage of an upright microscope with micromanipulators. A micropipette was filled with the solution containing plasmid DNA and TMRD and placed close to the cell body of CA1 pyramidal neurons. A stimulus consisting of 200 rectangular pulses at 200 Hz (30 V; 1 ms duration) was applied to the slice preparation. After electroporation, samples were maintained for an additional 2–4 d for green fluorescent protein (GFP) expression.

Imaging of organotypic slice culture. Live slice cultures were placed in a chamber containing Tyrode's solution for at least 1 h before the experiment. The chamber was maintained at 35°C and perfused at 0.5 ml/min with the same solution. A stimulation electrode was filled with Tyrode's solution and placed in the vicinity of GFP-positive dendrites (5–20 μm)

using a laser scanning differential interference contrast image and GFP fluorescence. Tetanic stimulation consisted of 100 pulses at 100 Hz (10 V; 0.1 ms duration). To evaluate direct depolarizing effects on dendrites, APV was applied at 150 μM in control experiments. This pharmacological manipulation completely suppressed the increase of spine volume after tetanic stimulation, indicating essential roles of postsynaptic NMDAR activation in spine enlargement.

Time-lapse imaging of live slice cultures was performed using a two-photon laser-scanning microscope (Radiance 2000MP; Bio-Rad), and GFP was excited at an excitation wavelength of 860 nm. A 60× water-immersion lens was used, and images were collected at additional digital zoom to obtain a nominal spatial resolution of 90 nm per pixel. Multiple optical sections were collected every 3 min. Under our imaging conditions, photobleaching of GFP and phototoxicity of two-photon excitation were not detectable.

Electrophysiology. Standard procedures were used to prepare hippocampal slices (400 μm thick) from male mice aged 7–10 weeks (Bongsebandhu-phubhakdi and Manabe, 2007). External solution contained the following (in mM): 119 NaCl, 2.5 KCl, 1.3 $MgSO_4$, 2.5 $CaCl_2$, 1.0 NaH_2PO_4, 26.2 $NaHCO_3$, 11 glucose, and 0.1 picrotoxin (a $GABA_A$ receptor antagonist). Synaptic responses were recorded from hippocampal slices at 25°C with extracellular field potential recordings in the stratum radiatum of the CA1 region, using a glass recording pipette filled with 3 M NaCl, or they were recorded with whole-cell voltage-clamp recordings from CA1 pyramidal neurons, using a patch pipette filled with the internal solution containing the following (in mM): 122.5 Cs gluconate, 17.5 CsCl, 10 HEPES, 0.2 EGTA, 8 NaCl, 2 Mg-ATP, and 0.3 Na_3-GTP, pH 7.2 and 290–310 mOsm. To evoke synaptic responses, Schaffer collateral/commissural fibers were stimulated at 0.1 Hz with a bipolar tungsten electrode. AMPAR-mediated EPSCs were recorded at −80 mV, and NMDAR-mediated EPSCs were recorded at +50 mV with the same stimulus strength in the presence of 10 μM 6-cyano-7-nitroquinoxaline-2,3-dione (CNQX) (a non-NMDAR antagonist). The baseline synaptic response was almost constant among experiments (initial slope values of EPSPs, 0.10–0.15 mV/ms; EPSCs amplitudes, 100–200 pA). For examining input–output relationships, a low concentration of CNQX (1 μM) was present to partially block AMPARs, which enables more accurate measurements, since the nonlinear summation of field EPSPs is reduced. An Axopatch-1D amplifier (Molecular Devices) was used to record synaptic responses. Data were digitized at 10 kHz and analyzed on-line and off-line using pClamp software (Molecular Devices).

Inhibitory avoidance. All mice used were male and 13–16 weeks of age at the time of training. They were accustomed to the experimenter by careful handling for >1 week before the start of the experiment. The procedure followed basically as described previously (Irvine et al., 2005). The mice were placed individually into the light compartment of a piece of inhibitory avoidance apparatus (O'HARA & Co.) facing away from the door. After 1 s, the door was opened, and the mice were allowed to enter the dark (shock) compartment. Once they entered the dark compartment after crossing with all four feet, the door was closed. The time to reach the middle of the dark compartment was measured automatically with infrared detection system (training latency). After a delay of 3 s, the mice received a mild footshock (125 V for 2 s, 0.2–0.4 mA). The footshock caused both wild-type and homozygous CaMKIIα (K42R) mice vocalization, urination, and bumping against the wall, demonstrating that the footshock was effective as an aversive stimulus to both genotypes. Ten seconds after the shock, they were removed from the apparatus and returned to the home cage. Twenty-four hours after training, the mice were again placed into the light compartment. The door was opened after 1 s, and the latency (maximum, 300 s) to enter the dark compartment was scored (test latency). To assess short-term memory, the mice were tested 40 min after training. In multitrial training, the mice were trained as described above, except that they were again placed in the light compartment after receiving a footshock. One second after the placement, the door was opened. If the mice reentered the dark compartment, the door was closed, and a footshock was again administered. Immediate learning after a single trial was assessed by comparing the latencies in the first and second trials (i.e., before and after the first shock). The training trials were repeated until the mice stayed in the light side for >120 s in a single trial. Twenty-four hours after multitrial training, the latency to enter the dark compartment was measured (maximum, 300 s). The behavior of the mice during training and tests was videotaped. Mice were excluded from the analysis if they took longer than 60 s to go into the dark compartment in the first training trial.

Data analysis. All data are expressed as mean ± SEM unless otherwise specified. Statistical analysis was performed by using *t* test, ANOVA followed by Fisher's PLSD test, Wilcoxon's signed rank test, or Mann–Whitney test.

Results

Generation of the CaMKIIα (K42R) knock-in mouse

To completely eliminate kinase activity of CaMKIIα, we took advantage of K42R mutation that prevents ATP binding necessary for phosphorylation reaction within the catalytic core of the enzyme, which is a standard procedure to inactivate various protein kinases (Taylor et al., 1990). Previous transfection experiments in cultures revealed that K42R mutation did not affect calmodulin-binding capacity of CaMKIIα, multimeric structure of the CaMKII holoenzyme, and activity-dependent postsynaptic translocation of CaMKIIα (Hanson et al., 1994; Mukherji and Soderling, 1994; Shen and Meyer, 1999). Using a CaMKIIα genomic fragment containing exon 2, we constructed a targeting vector containing nucleotide replacement for K42R mutation and generated the CaMKIIα (K42R) knock-in mouse (Fig. 1*A*). Homologous recombination was confirmed by Southern blot analyses (Fig. 1*B*), and genotypes were determined by PCR amplifying the loxP insertion site (Fig. 1*C*). Nucleotide replacement was confirmed by another PCR amplifying the mutation site followed by digestion with *Bst*NI (Fig. 1*D*) and further verified by nucleotide sequencing of the PCR products (Fig. 1*E*).

The genotypic distribution of the offspring obtained by crossing heterozygous mice followed Mendelian inheritance. Both heterozygous and homozygous K42R mice were hyperactive, but otherwise indistinguishable from wild-type mice. They were fertile and without any obvious neurological symptoms, except that mild limbic seizure was sporadically observed after 10 weeks of age, and that the survival rate in 6 months was lower compared with wild-type mice (wild type, 98.5%, 66 of 67; heterozygous, 95.2%, 159 of 167; homozygous, 78.8%, 67 of 85). Mice that showed any signs of seizure were excluded from the experiments.

Basic characterization of the CaMKIIα (K42R) knock-in mouse

Homozygous CaMKIIα (K42R) mice showed normal histological structures in adult brain sections examined by Nissl staining (data not shown). Their mRNA expression patterns of all isoforms (subunits) of CaMKII [i.e., CaMKIIα (neuron specific; the major forebrain isoform), CaMKIIβ (neuron specific; the second major forebrain and the major cerebellar isoform), CaMKIIγ and CaMKIIδ (non-neuron specific; minor isoforms)] were indistinguishable from those of wild-type mice, including dendritic mRNA localization of CaMKIIα in the hippocampus (Fig. 2*A*). Immunoblot analyses of forebrain and cerebellar homogenates revealed normal expression levels of all isoform proteins, except for a small decrease in CaMKIIα protein in the forebrain, in homozygous K42R mice (Fig. 2*B*, Table 1).

We next examined kinase activity of CaMKII in brain homogenates using a selective peptide substrate, autocamtide-2 (Fig. 2, compare *C*, *D*). Even in the forebrain from conventional CaMKIIα-null mice (Silva et al., 1992), about one-half of CaMKII activity was reported to be preserved, mainly because of the presence of intact CaMKIIβ activity. Consistent with such an

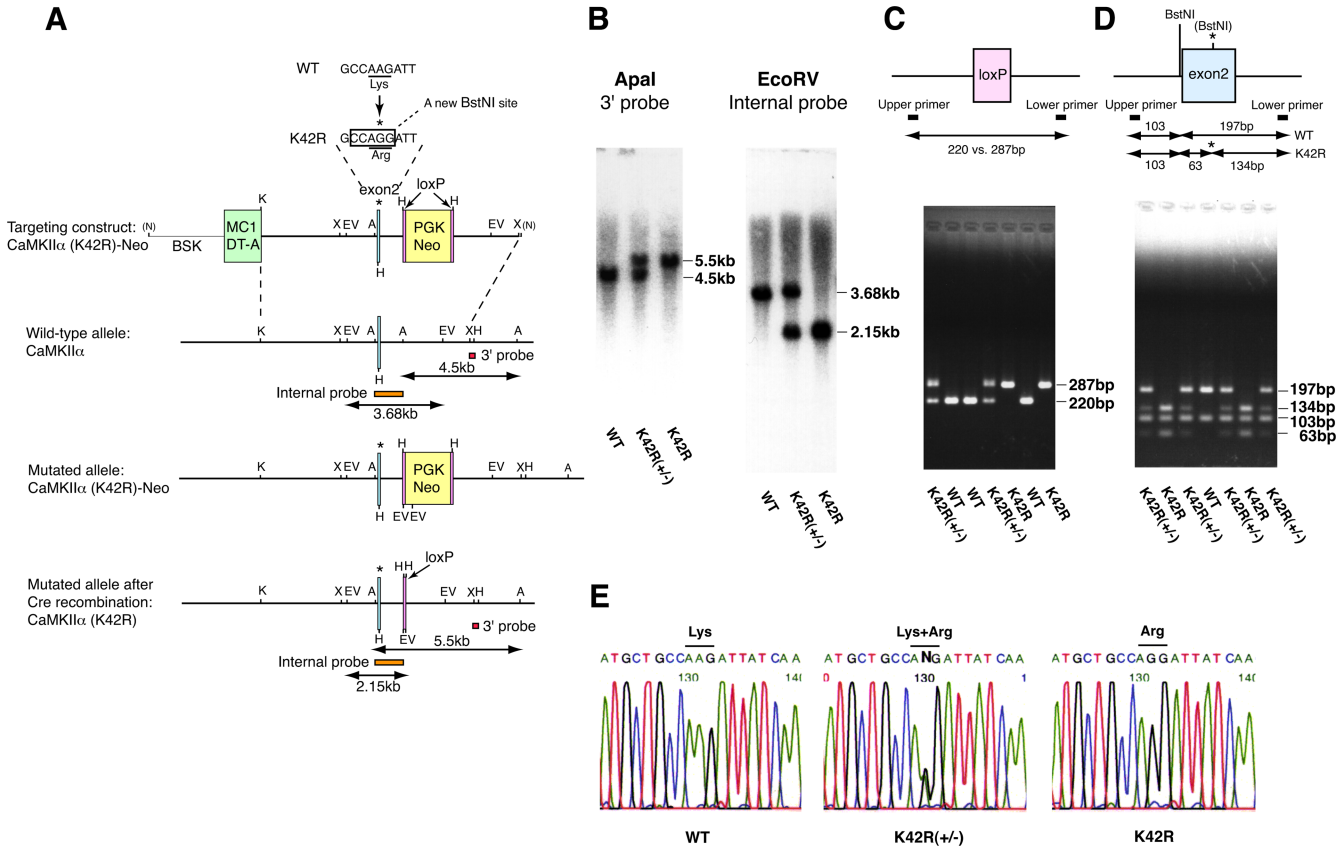

Figure 1. Generation of the CaMKIIα (K42R) knock-in mouse. ***A***, K42R mutation was introduced by replacing a nucleotide from AAG to AGG (* on top) within exon 2 of the CaMKIIα gene, which simultaneously generated a new restriction site for *Bst*NI. The homologously recombined ES clones after Cre recombination [CaMKIIα(K42R), bottom] were microinjected into eight-cell embryos to generate the K42R mouse. A, *Apa*I; BSK, pBluescript SK; EV, *Eco*RV; H, *Hin*dIII; K, *Kpn*I; N, *Not*I; X, *Xba*I. ***B***, Southern blot analyses of mouse genomic DNA to confirm homologous recombination. Mouse genomic DNA extracted from tails was digested by *Apa*I and hybridized with a 3′ external probe, or by *Eco*RV and with an internal probe. The positions of the probes are indicated in ***A***. K42R, Homozygous K42R mouse; K42R(+/−), heterozygous K42R mouse; WT, wild-type mouse. ***C***, Genotyping of the mouse by PCR amplifying the loxP insertion site to detect a 67 bp size shift. ***D***, Detection of a new *Bst*NI site (*) generated by nucleotide replacement for K42R mutation. The amplified PCR products containing the mutation site were digested by *Bst*NI. ***E***, Direct demonstration of the nucleotide replacement by sequencing the purified PCR products generated as in ***D***.

observation, we observed a 60–70% reduction in the total and Ca^{2+}/calmodulin-independent autonomous activity of CaMKII in the homozygous K42R forebrain, compared with wild-type control (Fig. 2*C*, left; Table 2). In the forebrain from heterozygous K42R mice, 75% of kinase activity was preserved (Fig. 2*C*, left; Table 2), and this moderate reduction was again comparable with that of CaMKIIα knock-out heterozygotes (Chapman et al., 1995) (Fig. 2*D*, left; Table 3). In the cerebellum in which CaMKIIβ predominates over CaMKIIα, no significant decrease was observed (Fig. 2*C*, right; Table 2). These results are consistent with the selective elimination of kinase activity of CaMKIIα within the CaMKII holoenzyme that shows compositional heterogeneity in specific brain regions.

The phospho-T286 level of CaMKIIα, a conventional indicator of the autonomous activity of CaMKIIα (Hudmon and Schulman, 2002; Lisman et al., 2002; Colbran and Brown, 2004), was reduced to 60% of the wild-type level in homozygous K42R forebrain (Fig. 2*B*, Table 1). The remaining T286 autophosphorylation seems to be derived from intact CaMKIIβ that can add phosphates to the adjacent inactive CaMKIIα within a CaMKII holoenzyme. The presence of a reduced, but certain level of T286 autophosphorylation in the K42R brain is a clear difference from previously reported T286A mice (Giese et al., 1998).

Since CaMKIIα is enriched in the PSD (Hudmon and Schulman, 2002; Lisman et al., 2002; Colbran and Brown, 2004), we examined the content of CaMKIIα in the PSD by immunoelectron microscopy (supplemental Fig. 1, available at www.jneurosci.org as supplemental material). Postembedding immunogold analysis in the stratum radiatum of the hippocampal CA1 region revealed that the number of immunogold particles for CaMKIIα, as well as that for PSD-95, a representative PSD protein, was indistinguishable between homozygous K42R and wild-type synapses, demonstrating that PSD association of CaMKIIα was intact in K42R mice.

Postsynaptic dynamics of CaMKIIα in cultured hippocampal neurons

We next performed a series of cell-biological studies using hippocampal cultured neurons to characterize the molecular properties of glutamatergic synapses with high resolution. Immunocytochemical staining of PSD-95 and Homer, representative postsynaptic proteins, revealed similar densities of protein clusters along dendrites in wild-type and homozygous K42R neurons (supplemental Fig. 2, available at www.jneurosci.org as supplemental material), indicating that the basic pattern of the development of the synapse was intact in K42R mice.

We then expressed GFP-labeled either wild-type or K42R-mutated CaMKIIα in neurons with respective genotypes and examined a synaptic turnover rate and activity-dependent postsynaptic translocation of CaMKIIα (Fig. 3). In neurons without stimulation, GFP-CaMKIIα showed diffuse distribution

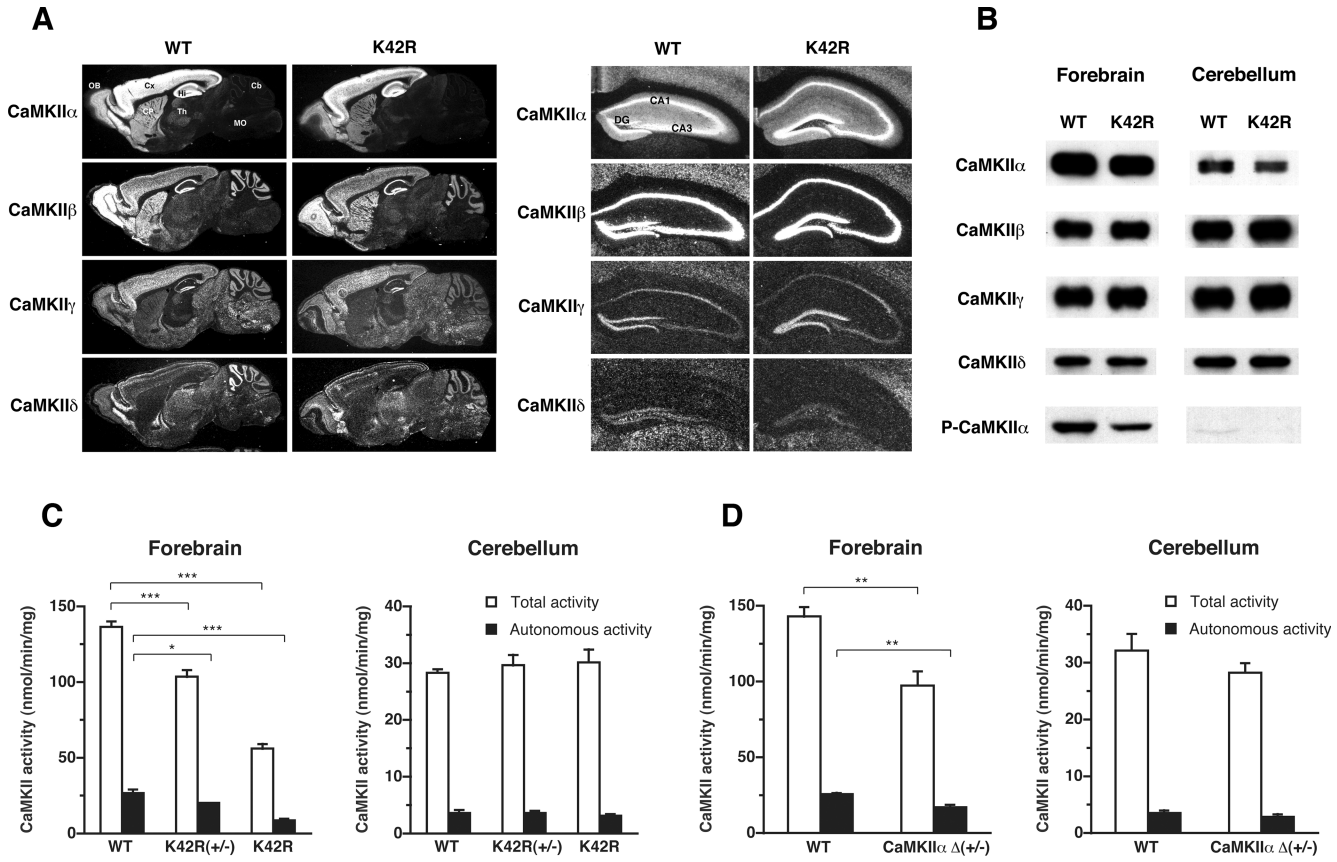

Figure 2. CaMKII isoform expression and CaMKII kinase activity in the CaMKIIα (K42R) knock-in mouse. ***A***, *In situ* hybridization showing the CaMKII isoform (CaMKIIα, β, γ, and δ) mRNA expression in adult brain sagittal sections (left) and hippocampal coronal sections (right) from wild-type (WT) and homozygous (K42R) mice. CA1–3, Subfield CA1–3 of Ammon's horn; Cb, cerebellum; CP, caudate–putamen; Cx, cerebral cortex; DG, dentate gyrus; Hi, hippocampal formation; MO, medulla oblongata; OB, olfactory bulb; Th, thalamus. ***B***, Immunoblot analyses showing the CaMKII isoform protein levels and the phospho-T286 level of CaMKIIα (P-CaMKIIα) in forebrain and cerebellar homogenates. See also Table 1. ***C***, CaMKII kinase activity in forebrain and cerebellar homogenates from wild-type (WT), heterozygous [K42R(+/−)], and homozygous (K42R) mice. Open columns, Total activity; filled columns, Ca^{2+}/calmodulin-independent autonomous activity. Error bars indicate SEM. ***$p < 0.0001$, *$p < 0.05$, ANOVA followed by Fisher's PLSD test ($n = 5$). See also Table 2. ***D***, CaMKII kinase activity in heterozygous CaMKIIα knock-out mice [CaMKIIα Δ(+/−)] for comparison. **$p < 0.01$, *t* test ($n = 4$). See also Table 3. The CaMKIIα protein level in heterozygous knock-out mice was 39.8 ± 5.3% ($p < 0.001$, forebrain) and 49.5 ± 15.3% ($p < 0.05$, cerebellum) of the wild-type level (one-group *t* test, $n = 5$).

Table 1. CaMKII isoform protein levels and phospho-T286 level in brain homogenates from homozygous CaMKIIα (K42R) mice compared with wild-type mice

	Forebrain (% of WT)	Cerebellum (% of WT)
CaMKIIα	78.7 ± 6.2*	109.5 ± 23.4
CaMKIIβ	108.4 ± 4.3	101.3 ± 14.7
CaMKIIγ	137.2 ± 39.7	93.9 ± 17.5
CaMKIIδ	103.5 ± 17.9	100.2 ± 11.0
Phospho-T286-CaMKIIα	63.4 ± 12.0*	n.d.[a]

Quantitative data were obtained by immunoblot analyses as represented in Figure 2*B*.

[a]Phospho-T286-CaMKIIα level in the cerebellum was too low to quantify accurately.

*Significantly different from wild-type (WT) levels: $p < 0.05$ (one group *t* test), $n = 5$.

Table 2. Relative CaMKII kinase activity in brain homogenates from homozygous and heterozygous CaMKIIα (K42R) mice compared with wild-type mice

	Forebrain (% of WT)		Cerebellum (% of WT)	
	K42R	K42R(+/−)	K42R	K42R(+/−)
Total activity	41.0 ± 1.6	75.9 ± 2.9	106.5 ± 8.0	104.8 ± 6.9
Autonomous activity	31.9 ± 2.7	75.6 ± 4.1	96.6 ± 17.3	105.2 ± 14.7

CaMKII kinase activity in mutant mice shown in Figure 2*C* is expressed as a percentage of that in wild-type (WT) mice in the same preparation group ($n = 5$).

Table 3. Relative CaMKII kinase activity in brain homogenates from heterozygous CaMKIIα knock-out mice compared with wild-type mice

	Forebrain (% of WT)	Cerebellum (% of WT)
	CaMKIIα Δ(+/−)	CaMKIIα Δ(+/−)
Total activity	68.5 ± 7.4	90.3 ± 10.6
Autonomous activity	67.1 ± 7.9	83.8 ± 12.7

CaMKII kinase activity in mutant mice shown in Figure 2*D* is expressed as a percentage of that in wild-type (WT) mice in the same preparation group ($n = 4$).

throughout the soma and neurites (Fig. 3*A*,*D*). This distributional pattern was consistent with previous reports (Shen and Meyer, 1999; Shen et al., 2000; Hudmon et al., 2005) and was preserved in homozygous K42R neurons. A steady-state turnover rate of CaMKIIα in dendritic spines was measured by using FRAP (Fig. 3*A*,*B*). The recovery rate of GFP-CaMKIIα on spines was slightly enhanced in K42R neurons (Fig. 3*B*). This increased mobility cannot be attributed to general enhancement of protein mobility in spines, as the recovery rate of GFP-Homer1c was indistinguishable between the genotypes (Fig. 3*C*).

Next, we examined activity-dependent postsynaptic translocation of CaMKIIα by using caged glutamate in wild-type and homozygous K42R neurons (Fig. 3*D–F*). Glutamate uncaging induced translocation of GFP-CaMKIIα to dendritic spines with a faster time course in K42R neurons (Fig. 3*D*,*E*). The time constant of CaMKIIα accumulation in homozygous K42R neurons

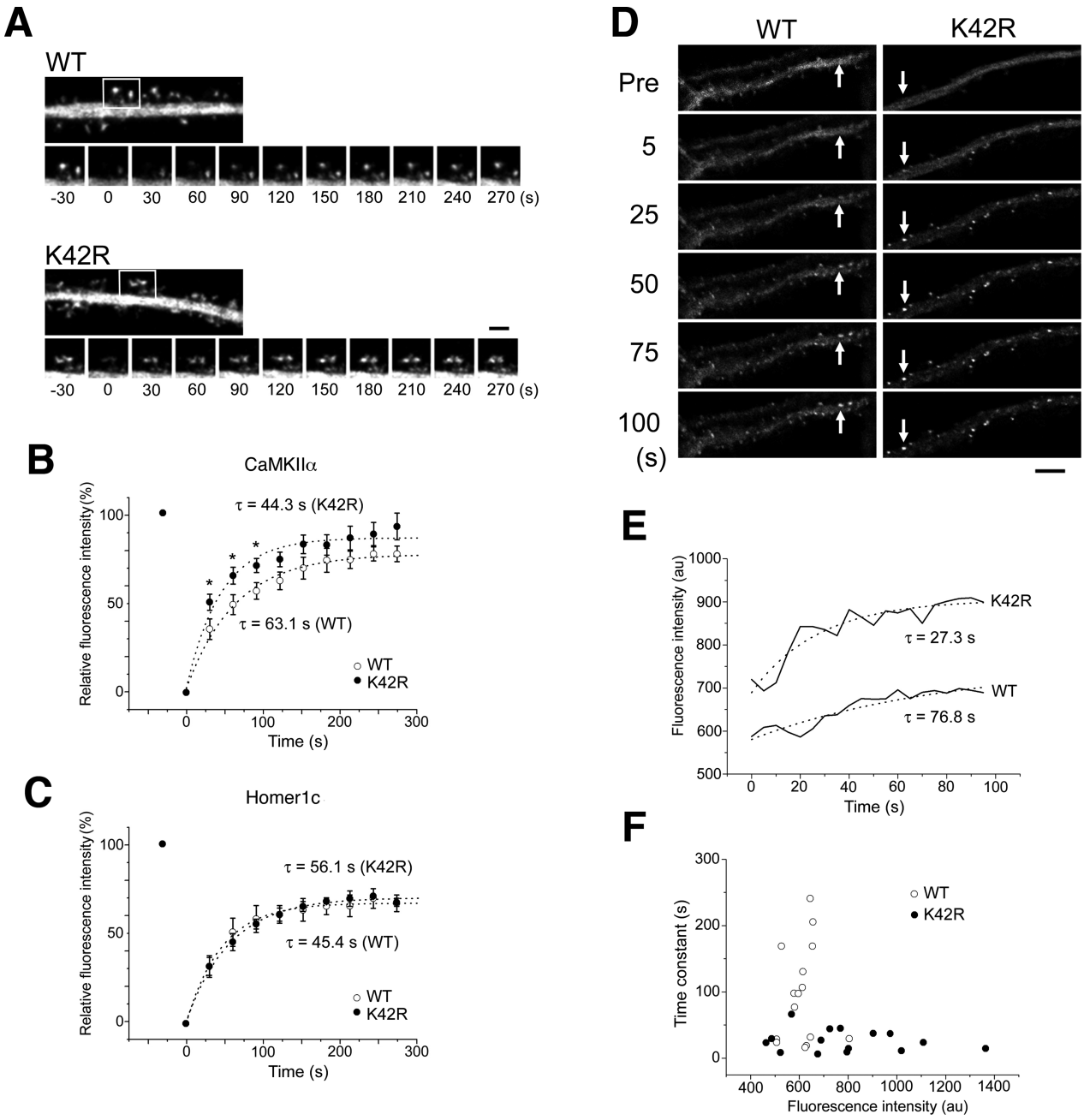

Figure 3. Postsynaptic dynamics of CaMKIIα in CaMKIIα (K42R) neurons. ***A***, FRAP analysis of wild-type and K42R-mutated CaMKIIα tagged with GFP and expressed in hippocampal neurons with respective genotypes. Scale bar, 3 μm. ***B***, FRAP analysis revealed a reduced time constant of K42R CaMKIIα with enhanced fluorescence recovery at the initial three time points (30, 60, and 90 s after bleaching). *$p < 0.05$, *t* test. Open circles, Wild type, $n = 17$ cells; filled circles, K42R, $n = 17$; three independent preparations from each genotype. Error bars indicate SEM. ***C***, Fluorescence recovery of GFP-Homer1c (wild type, $n = 6$ cells; K42R, $n = 6$; one independent preparation from each genotype). ***D***, Local dendritic stimulation by caged glutamate revealed faster translocation of K42R CaMKIIα. The arrows indicate the CaMKIIα clusters analyzed in ***E***. Scale bar, 5 μm. ***E***, Time course of CaMKIIα accumulation induced by glutamate uncaging. Time constants of CaMKIIα accumulation were estimated by exponential fittings. Smaller time constants were observed in homozygous K42R neurons than in wild-type neurons. ***F***, A plot of average time constant against relative fluorescence intensity within dendrites. Open circles, Wild type, $n = 15$ cells; filled circles, K42R, $n = 15$; three independent preparations from each genotype.

was significantly smaller than that in wild-type neurons (wild type, 96.2 ± 19.0 s, $n = 15$; K42R, 26.5 ± 4.4 s, $n = 15$; $p < 0.01$, *t* test) (Fig. 3*E*). The difference in time constant was independent of the efficiency of transfection, as there was no correlation between time constant and fluorescence intensity (Fig. 3*F*). Thus, activity-dependent postsynaptic translocation of CaMKIIα was preserved and rather enhanced in K42R neurons. The result is consistent with a previous observation using rat hippocampal neurons that K42R mutation did not impair postsynaptic translocation of CaMKIIα (Shen and Meyer, 1999). Faster translocation of CaMKIIα in K42R neurons may be attributable to the decreased phospho-T286 level (Fig. 2*B*, Table 1), as a previous study reported that T286A mutation accelerated postsynaptic translocation of CaMKIIα (Hudmon et al., 2005).

Tetanus-induced spine structural plasticity in organotypic hippocampal slices

The above study clearly demonstrates that, in homozygous K42R neurons, CaMKIIα can be mobilized to synaptic sites in an activity-dependent manner. To see whether structural remodel-

ing of dendritic spines associated with LTP was also preserved in K42R neurons, we next examined tetanus-induced spine dynamics by two-photon time-lapse microscopy in GFP-expressing hippocampal pyramidal neurons from slice cultures (Fig. 4). In wild-type slices, tetanic stimulation (100 Hz; 1 s) induced a robust and sustained enlargement of dendritic spines on pyramidal neurons in the CA1 region (Fig. 4*A*, top). However, such a stimulus-dependent spine remodeling was severely impaired in homozygous K42R neurons (Fig. 4*A*, bottom), in both the early phase (<5 min) and the late maintenance phase (5–20 min) of spine volume increase (Fig. 4*B*). The extent of spine volume increase in the late maintenance phase estimated by the average of total fluorescence increase of spines at the last three time points (16, 19, and 22 min after tetanic stimulation) was significantly suppressed in K42R neurons, compared with wild-type neurons (wild type, 126.5 ± 5.9% of baseline, $n = 85$; K42R, 102.4 ± 3.3%, $n = 73$; $p < 0.01$, *t* test). Examination of individual time-lapse sequences revealed that a small number of K42R spines showed an enlargement of their size in the early phase. However, this specific subset of K42R spines failed to sustain spine enlargement in the late phase (Fig. 4*C*). Thus, spines with mutated CaMKIIα that lacks kinase activity but preserves its postsynaptic association and translocational ability failed to respond to afferent stimulation that was sufficient to induce structural plasticity in wild-type spines.

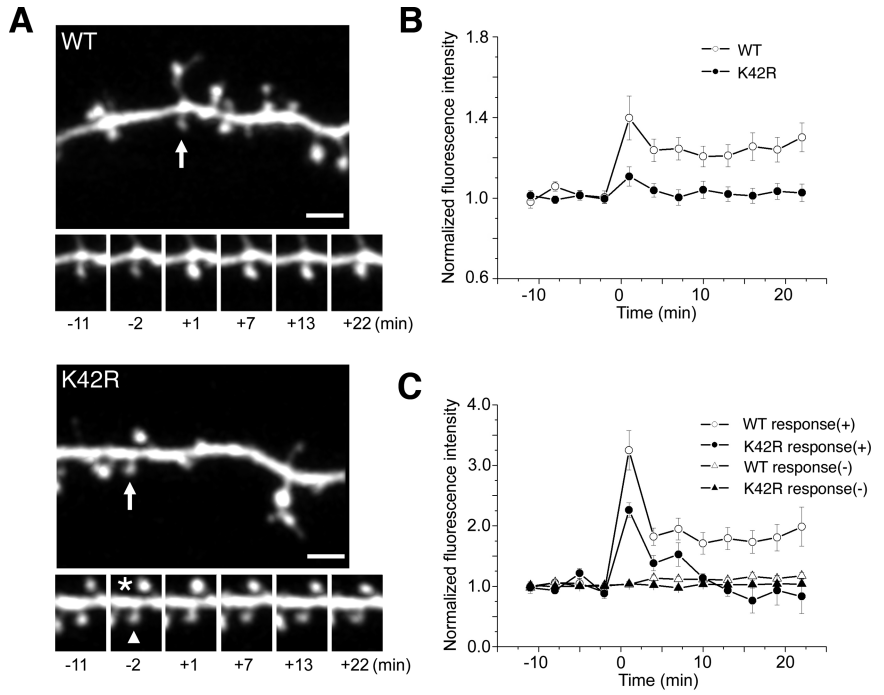

Figure 4. Impaired spine structural plasticity in CaMKIIα (K42R) neurons. ***A***, Extracellular stimulation (100 Hz; 1 s) of GFP-expressing CA1 pyramidal neuronal dendrites in organotypic hippocampal slices from wild-type or homozygous K42R mice. The bottom time-lapse images show structural change of spines (arrows in top images) after electrical stimulation. Spine volume increase was either undetectable (arrowhead) or transient (asterisk) in a K42R neuron. Scale bars, 2 μm. ***B***, Quantification of total fluorescence intensity of spines before and after tetanic stimulation at $t = 0$. Total fluorescence intensity was normalized by the average of fluorescence intensities before tetanic stimulation. Activity-dependent spine enlargement was severely impaired in K42R neurons. Open circles, Wild type, $n = 85$ spines (6 slice preparations); filled circles, K42R, $n = 73$ (9 slice preparations). Error bars indicate SEM. ***C***, Quantification of total fluorescence intensity in spines classified by their immediate response after tetanic stimulation. Spines with a more than twofold increase of total fluorescence intensity at $t = 1$ min were classified as response (+) (circles), and the other spines were classified as response (−) (triangles) [wild-type response (+), $n = 14$ spines; K42R response (+), $n = 4$; wild-type response (−), $n = 71$; K42R response (−), $n = 69$].

Tetanus-induced LTP in acute hippocampal slices

Since the above study revealed defects in structural plasticity at the individual spine level in K42R mice, we next examined functional synaptic plasticity at the Schaffer collateral–CA1 synapse by electrophysiological experiments using acute hippocampal slices (Fig. 5). Basal synaptic transmission was intact in K42R mice, as revealed by indistinguishable input–output relationship of AMPAR-mediated excitatory synaptic transmission between the genotypes (Fig. 5*A*). The ratio of NMDAR-mediated EPSCs/AMPAR-mediated EPSCs was also unchanged (wild type, 62.8 ± 4.7%, $n = 8$ cells; K42R, 67.9 ± 3.8%, $n = 9$; $p > 0.05$, *t* test) (Fig. 5*B*), indicating that the properties of NMDARs in K42R mice were intact. In addition, two forms of presynaptic short-term plasticity, paired-pulse facilitation (PPF) (Fig. 5*C*) and posttetanic potentiation (PTP) (Fig. 5*D*), were both indistinguishable between the genotypes, suggesting that the fundamental presynaptic functions are normal. However, LTP was severely impaired in K42R mice (Fig. 5*E*). Tetanic stimulation (100 Hz, 1 s) induced robust LTP in wild-type mice (156.5 ± 5.6% of baseline at 50–60 min after tetanic stimulation; $p < 0.0001$; $n = 10$ slices; paired *t* test), whereas virtually no LTP was induced in homozygous K42R mice (106.1 ± 2.8%; $p > 0.05$; $n = 10$; paired *t* test). The difference between the genotypes was significant ($p < 0.0001$; unpaired *t* test). When the same tetanus was repeated (100 Hz; 1 s, four times; 10 s intertetanus interval), larger LTP was observed in wild-type mice (170.8 ± 9.1% of baseline; $p < 0.001$; $n = 7$ slices; paired *t* test), whereas only slight potentiation was observed in K42R mice (130.7 ± 8.8%; $p < 0.05$; $n = 6$; paired *t* test) (supplemental Fig. 3, available at www.jneurosci.org as supplemental material). The potentiation ratio in K42R mice was significantly smaller than that in wild-type mice ($p < 0.05$, unpaired *t* test). LTP induced by repetitive tetanic stimulation in both genotypes was completely blocked in the presence of the NMDAR antagonist, D-2-amino-5-phosphonovaleric acid (D-APV, 50 μM) (wild type, 106.3 ± 2.7% of baseline, $p > 0.05$, $n = 9$; K42R, 102.2 ± 2.3%, $p > 0.05$, $n = 8$, paired *t* test). Thus, NMDAR-dependent LTP induction at the Schaffer collateral–CA1 synapse was severely impaired in K42R mice.

Inhibitory avoidance learning

The above study clearly demonstrates that kinase activity of CaMKIIα is essential for both structural and functional expression of synaptic plasticity in the hippocampus. To further examine the role of kinase activity of CaMKIIα at the behavioral level, we next studied one-trial inhibitory avoidance learning, a form of memory that is dependent on the hippocampus (Lorenzini et al., 1996; Impey et al., 1998; Izquierdo et al., 2006) (Fig. 6). Wild-type mice showed clear avoidance memory 24 h after one-trial training (i.e., they stayed in the light compartment as long as the cutoff latency of 300 s) (Fig. 6*A*). However, homozygous K42R mice

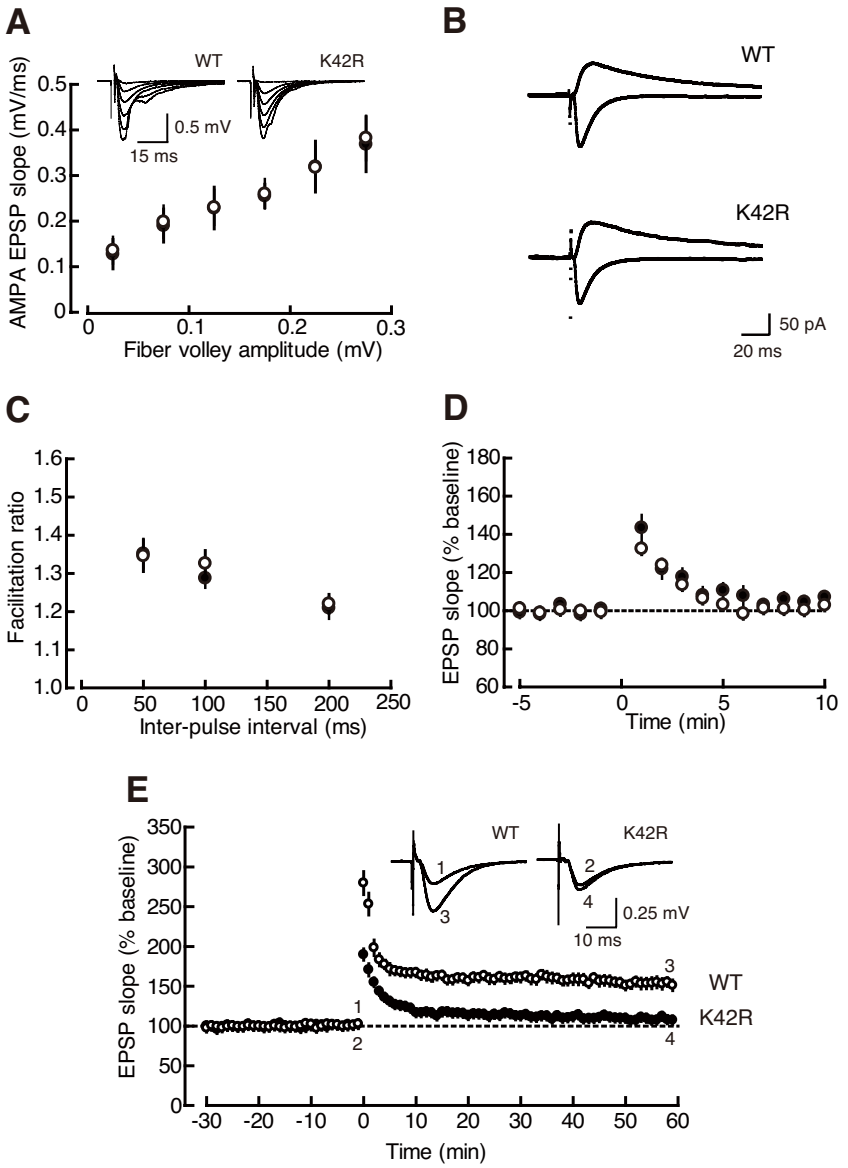

Figure 5. LTP was severely impaired in CaMKIIα (K42R) mice. ***A***, The input–output relationships of AMPAR-mediated EPSPs of wild-type (open circles; $n = 12$ slices) and homozygous K42R slices (filled circles; $n = 10$). Error bars indicate SEM. ***B***, AMPAR-mediated (downward traces) and NMDAR-mediated EPSCs (upward traces) in wild-type and homozygous K42R neurons. ***C***, PPF recorded as a function of the interstimulus intervals in the presence of 25 μM D-APV (wild type, $n = 8$ slices; K42R, $n = 8$). ***D***, PTP induced by a train of high-frequency stimuli (100 Hz; 1 s) in the presence of 50 μM D-APV (wild type, $n = 10$ slices; K42R, $n = 8$). ***E***, The time course of LTP induced by single tetanic stimulation (100 Hz; 1 s). Representative traces (averaged 10 consecutive responses) in the inset are EPSPs obtained at the times indicated by the numbers in the graph (wild type, $n = 10$ slices; K42R, $n = 10$). Robust LTP was induced in wild-type slices, whereas no LTP was observed in K42R slices.

entered the dark (shock) compartment without hesitation 24 h after training (Fig. 6*B*), indicating that no avoidance memory was formed. When another groups of mice were tested 40 min after training, wild-type mice again refrained from entering the dark compartment (Fig. 6*C*), whereas K42R mice did enter (Fig. 6*D*), indicating that short-term memory was also impaired in K42R mice.

To further examine whether learning itself or memory retention was impaired, we next examined immediate learning in K42R mice by using multitrial training (Fig. 6*E–G*). The latencies in the first and second trials (before and after the first shock) did not differ significantly (Fig. 6*E*), indicating that learning itself was impaired in K42R mice. However, after repeated exposure to the shock chamber in multitrial training, K42R mice eventually refrained from entering the dark compartment (Fig. 6*F*). When tested 24 h after multitrial training, K42R mice showed avoidance behavior to some extent (Fig. 6*G*), which was still impaired compared with wild-type mice after one-trial training (compare with Fig. 6*A*, right). These results demonstrate that, in addition to synaptic plasticity, behavioral learning was indeed severely impaired in the absence of kinase activity of CaMKIIα.

Discussion

In this study, we critically evaluated enzymatic roles of CaMKIIα in long-term synaptic plasticity and behavioral learning by using the CaMKIIα (K42R) knock-in mouse that lacks kinase activity of CaMKIIα. The K42R mouse is different from previously reported CaMKIIα mutant mice that showed reduced kinase activity in a number of ways. First, it differs from the CaMKIIα-null mouse (Silva et al., 1992) in that both mRNA and protein expressions of CaMKIIα are fairly well preserved. There was a small decrease in the total CaMKIIα protein level in the homozygous K42R forebrain (~20%) (Table 1). However, the extent of the decrease was even less than that in the heterozygous knock-out forebrain (~60%) (Fig. 2*D*, legend). The small decrease in the K42R brain could be derived from either reduced transcription because of the remaining loxP site (Fig. 1*A*) or possible instability of the mutated protein. Second, the K42R mouse differs from the T286A mouse (Giese et al., 1998) in that not only the autonomous activity but also the Ca^{2+}/calmodulin-dependent activity is completely lacking and in that T286 autophosphorylation can occur to some extent by adjacent intact CaMKIIβ within a holoenzyme. Third, it differs from the T305D mouse (Elgersma et al., 2002) in that Ca^{2+}/calmodulin-binding capacity and PSD association of CaMKIIα are not altered. Thus, we could extract the consequences of the lack of kinase activity of CaMKIIα with its other protein functions mostly intact by using K42R mice.

Consistent with previous transfection studies (Shen and Meyer, 1999), elimination of kinase activity of CaMKIIα in mice did not block its activity-dependent postsynaptic translocation (Fig. 3*D*,*E*). Immunoelectron microscopic examination also revealed the unaltered content of CaMKIIα, as well as that of PSD-95, in the PSD (supplemental Fig. 1, available at www.jneurosci.org as supplemental material). Normal association of CaMKIIα and its robust translocation to the PSD on synaptic activation support the notion that molecular elements necessary for PSD remodeling after high-frequency stimulation are mostly preserved in K42R mice. This

property is unique, compared with altered contents of CaMKIIα in the PSD of the mutant mice with point mutations at T305/306 within the calmodulin-binding region (Elgersma et al., 2002). Previous transfection studies had indicated that Ca^{2+}/calmodulin binding is a key regulatory mechanism for postsynaptic translocation of CaMKIIα (Shen and Meyer, 1999) and that T305/306 autophosphorylation promotes detachment of CaMKIIα from postsynaptic sites (Shen et al., 2000). Indeed, T305D mice, whose mutation blocks Ca^{2+}/calmodulin binding, showed decreased CaMKIIα content in the PSD and severely impaired LTP (Elgersma et al., 2002). In addition, TT305/306VA mice, whose mutation prevents T305/306 autophosphorylation, showed increased CaMKIIα content in the PSD and reduced threshold for LTP (Elgersma et al., 2002). Thus, not only kinase activity of CaMKIIα but also intracellular localization of CaMKIIα seems to have a profound effect on postsynaptic functions of CaMKIIα. As for K42R mice, even with normal association of CaMKIIα to the PSD and its translocational ability, high-frequency stimulation failed to induce long-lasting spine volume increase (Fig. 4), as well as LTP (Fig. 5*E*), indicating an essential role of kinase activity of CaMKIIα at postsynaptic sites to initiate these processes (Fig. 7).

Such a drastic downregulation of postsynaptic plasticity in the absence of kinase activity of CaMKIIα is in contrast to recent observations indicating a nonenzymatic role of CaMKIIα in short-term presynaptic plasticity. Enhanced presynaptic plasticity was reported in the CaMKIIα-null mouse (Hinds et al., 2003; Hojjati et al., 2007), but not in any of CaMKIIα knock-in mice (T286A, T305D and TT305/306VA) and not by pharmacological inhibition of kinase activity (Hojjati et al., 2007). Consistent with such observations, PPF and PTP, two forms of presynaptic short-term plasticity, were not altered in K42R mice (Fig. 5*C*,*D*), which is a clear contrast to altered PPF and PTP observed in CaMKIIα-null mice (Chapman et al., 1995). More detailed studies would be necessary, however, to determine whether the effect of CaMKIIα on presynaptic plasticity is indeed nonenzymatic.

Can kinase activity of CaMKIIα explain all the features of postsynaptic expression of plasticity? Defects in spine structural plasticity observed in K42R mice are consistent with previous studies reporting that pharmacological blockade of kinase activity of CaMKII was effective in preventing persistent enlargement of dendritic spines (Matsuzaki et al., 2004; Honkura et al., 2008). However, other studies reported that persistent spine volume increase was associated with postsynaptic accumulation of CaMKIIα (Otmakhov et al., 2004; Zhang et al., 2008), indicating a role of CaMKIIα as a scaffold at postsynaptic sites. Indeed, CaMKIIα can bind a number of postsynaptic proteins including itself (Colbran and Brown, 2004; Hudmon et al., 2005) and may be an ideal molecule as a postsynaptic scaffold. In

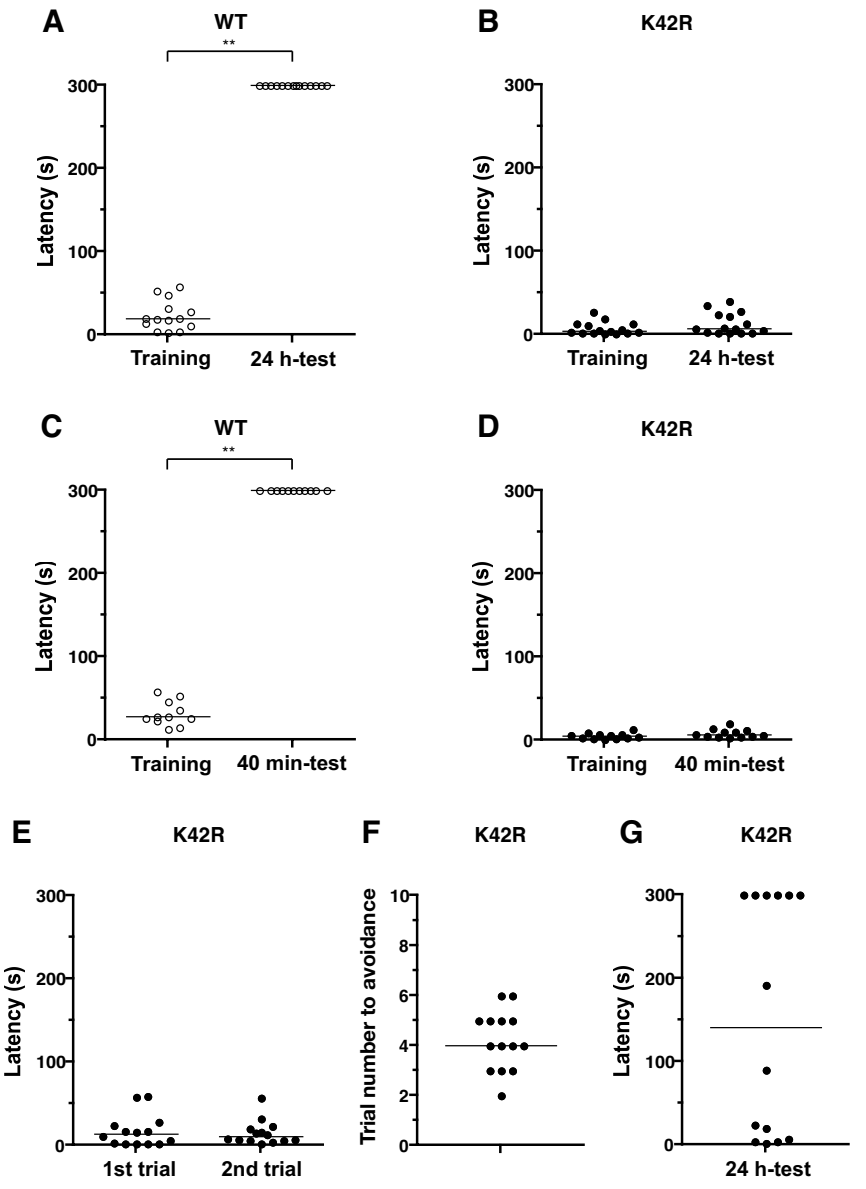

Figure 6. Inhibitory avoidance learning was severely impaired in CaMKIIα (K42R) mice. ***A***, Wild-type mice showed increased step-through latency compared with training latency, when tested 24 h after one-trial training in the inhibitory avoidance task. Cutoff latency was set at 300 s. Bars represent median. $^{**}p < 0.01$, Wilcoxon's signed rank test ($n = 14$). ***B***, Homozygous K42R mice showed no difference between training and 24 h latencies, indicating that avoidance memory was severely impaired in K42R mice ($n = 15$). Note that shorter training latency in K42R mice (***B***, left) than in wild-type mice (***A***, left) reflected hyperactivity in K42R mice ($p < 0.01$, Mann–Whitney test). ***C***, Short-term memory was tested 40 min after training. Wild-type mice showed increased latency after 40 min, compared with training latency. $^{**}p < 0.01$, Wilcoxon's signed rank test ($n = 11$). ***D***, Homozygous K42R mice showed no difference between training and 40 min latencies, indicating that short-term memory was also severely impaired in K42R mice ($n = 12$). ***E***, Multitrial training was performed to examine immediate learning in homozygous K42R mice. K42R mice that had been subjected to one-trial training and tested 24 h memory in ***B*** were retrained after an interval of 5–15 d. The latencies in the first trial (before the first shock) and the second trial (after the first shock) were not different, indicating that immediate learning after a single trial was impaired in K42R mice ($n = 14$). ***F***, The number of trials necessary for homozygous K42R mice to show immediate avoidance in multitrial training. Training trials were repeated until the mice stayed in the light side for >120 s in a single trial. ***G***, When tested 24 h after multitrial training, homozygous K42R mice showed increased step-through latency compared with the first training latency (***E***, left) ($p < 0.05$, Wilcoxon's signed rank test). Note that the 24 h latency after multitrial training in K42R mice (***G***) was significantly shorter than the 24 h latency after single-trial training in wild-type mice (***A***, right) ($p < 0.01$, Mann–Whitney test).

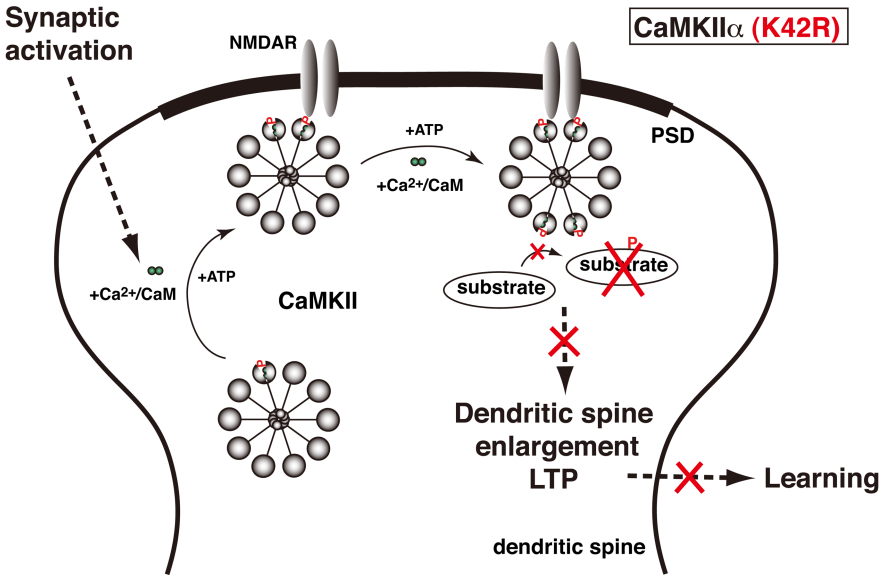

Figure 7. Schematic illustration showing that kinase activity of CaMKIIα is essential for structural, functional, and behavioral expression of synaptic memory. Strong synaptic activation induces activation of CaMKII by binding of Ca^{2+}/calmodulin (Ca^{2+}/CaM) and the following postsynaptic translocation of CaMKII. Activated CaMKII undergoes T286 autophosphorylation to generate the autonomous activity and phosphorylates substrate proteins to initiate dendritic spine enlargement and LTP. Such synaptic plasticity seems to be a basis for behavioral expression of learning and memory *in vivo*. In the kinase-dead CaMKIIα (K42R) knock-in mouse, mutated CaMKIIα did undergo postsynaptic translocation on synaptic activation, and T286 autophosphorylation could occur to some extent by adjacent intact CaMKIIβ within a CaMKII holoenzyme. However, mutated CaMKIIα cannot phosphorylate substrate proteins, and thus, both prolonged dendritic spine enlargement and LTP were not induced. Hippocampus-dependent learning was also impaired in the CaMKIIα (K42R) mouse. These results demonstrate an indispensable role of CaMKIIα kinase activity in dendritic spine enlargement, LTP, and learning.

addition, CaMKIIβ, the other neuron-specific subunit within a CaMKII holoenzyme, may also play such a scaffolding role in spine structural plasticity. CaMKIIβ, but not CaMKIIα, has actin-binding capacity and morphogenic activity in spine development (Fink et al., 2003; Okamoto et al., 2007), and remodeling of the actin cytoskeleton seems to be critical for long-lasting enlargement of dendritic spines (Okamoto et al., 2004; Honkura et al., 2008). Thus, our results do not rule out a possibility of additional roles of CaMKIIα as a scaffold on the postsynaptic side in the maintenance of structural and functional synaptic plasticity after initial phosphorylation of postsynaptic proteins. Nevertheless, the analyses presented here revealed an unambiguous role of CaMKIIα kinase activity in the initiation of spine structural plasticity and LTP.

Another interesting finding in this study is a possible correlation between LTP and a form of learning that can be established in a single trial. Involvement of hippocampal LTP in inhibitory avoidance learning has been suggested (Izquierdo et al., 2006), and a recent study reported that avoidance training actually caused LTP in the CA1 region of the hippocampus (Whitlock et al., 2006). Activation of CaMKIIα was also reported after avoidance training in the CA1 region (Cammarota et al., 2008). Consistent with such observations, K42R mice showed no LTP by a single tetanus in slice experiments (Fig. 5*E*) and no learning in the one-trial inhibitory avoidance task (Fig. 6*A–D*). After repeated training trials, however, K42R mice did show a certain level of avoidance (Fig. 6*G*), just as repeated tetani could cause slight potentiation in K42R slices (supplemental Fig. 3, available at www.jneurosci.org as supplemental material). Similar deficits in both LTP and inhibitory avoidance learning in K42R mice may suggest a common signal transduction pathway shared by synaptic plasticity and behavioral learning. Thus, the K42R mice described in this study could be a powerful tool to further examine the relationship between the two processes and to identify downstream molecular details in memory formation *in vivo*.

References

Bliss TV, Collingridge GL (1993) A synaptic model of memory: long-term potentiation in the hippocampus. Nature 361:31–39.

Bongsebandhu-phubhakdi S, Manabe T (2007) The neuropeptide nociceptin is a synaptically released endogenous inhibitor of hippocampal long-term potentiation. J Neurosci 27:4850–4858.

Cammarota M, Bevilaqua LR, Rossato JI, Lima RH, Medina JH, Izquierdo I (2008) Parallel memory processing by the CA1 region of the dorsal hippocampus and the basolateral amygdala. Proc Natl Acad Sci U S A 105:10279–10284.

Chapman PF, Frenguelli BG, Smith A, Chen CM, Silva AJ (1995) The α-Ca^{2+}/calmodulin kinase II: a bidirectional modulator of presynaptic plasticity. Neuron 14:591–597.

Colbran RJ, Brown AM (2004) Calcium/calmodulin-dependent protein kinase II and synaptic plasticity. Curr Opin Neurobiol 14:318–327.

Derkach V, Barria A, Soderling TR (1999) Ca^{2+}/calmodulin-kinase II enhances channel conductance of α-amino-3-hydroxy-5-methyl-4-isoxazolepropionate type glutamate receptors. Proc Natl Acad Sci U S A 96:3269–3274.

Elgersma Y, Fedorov NB, Ikonen S, Choi ES, Elgersma M, Carvalho OM, Giese KP, Silva AJ (2002) Inhibitory autophosphorylation of CaMKII controls PSD association, plasticity, and learning. Neuron 36:493–505.

Fink CC, Bayer KU, Myers JW, Ferrell JE Jr, Schulman H, Meyer T (2003) Selective regulation of neurite extension and synapse formation by the β but not the α isoform of CaMKII. Neuron 39:283–297.

Fukaya M, Watanabe M (2000) Improved immunohistochemical detection of postsynaptically located PSD-95/SAP90 protein family by protease section pretreatment: a study in the adult mouse brain. J Comp Neurol 426:572–586.

Giese KP, Fedorov NB, Filipkowski RK, Silva AJ (1998) Autophosphorylation at Thr286 of the alpha calcium-calmodulin kinase II in LTP and learning. Science 279:870–873.

Haas K, Sin WC, Javaherian A, Li Z, Cline HT (2001) Single-cell electroporation for gene transfer in vivo. Neuron 29:583–591.

Hanson PI, Kapiloff MS, Lou LL, Rosenfeld MG, Schulman H (1989) Expression of a multifunctional Ca^{2+}/calmodulin-dependent protein kinase and mutational analysis of its autoregulation. Neuron 3:59–70.

Hanson PI, Meyer T, Stryer L, Schulman H (1994) Dual role of calmodulin in autophosphorylation of multifunctional CaM kinase may underlie decoding of calcium signals. Neuron 12:943–956.

Harvey CD, Svoboda K (2007) Locally dynamic synaptic learning rules in pyramidal neuron dendrites. Nature 450:1195–1200.

Hayashi Y, Shi SH, Esteban JA, Piccini A, Poncer JC, Malinow R (2000) Driving AMPA receptors into synapses by LTP and CaMKII: requirement for GluR1 and PDZ domain interaction. Science 287:2262–2267.

Hinds HL, Tonegawa S, Malinow R (1998) CA1 long-term potentiation is diminished but present in hippocampal slices from α-CaMKII mutant mice. Learn Mem 5:344–354.

Hinds HL, Goussakov I, Nakazawa K, Tonegawa S, Bolshakov VY (2003) Essential function of α-calcium/calmodulin-dependent protein kinase II in neurotransmitter release at a glutamatergic central synapse. Proc Natl Acad Sci U S A 100:4275–4280.

Hojjati MR, van Woerden GM, Tyler WJ, Giese KP, Silva AJ, Pozzo-Miller L, Elgersma Y (2007) Kinase activity is not required for αCaMKII-dependent presynaptic plasticity at CA3-CA1 synapses. Nat Neurosci 10:1125–1127.

Honkura N, Matsuzaki M, Noguchi J, Ellis-Davies GC, Kasai H (2008) The

subspine organization of actin fibers regulates the structure and plasticity of dendritic spines. Neuron 57:719–729.

Hudmon A, Schulman H (2002) Neuronal Ca^{2+}/calmodulin-dependent protein kinase II: the role of structure and autoregulation in cellular function. Annu Rev Biochem 71:473–510.

Hudmon A, Lebel E, Roy H, Sik A, Schulman H, Waxham MN, De Koninck P (2005) A mechanism for Ca^{2+}/calmodulin-dependent protein kinase II clustering at synaptic and nonsynaptic sites based on self-association. J Neurosci 25:6971–6983.

Impey S, Smith DM, Obrietan K, Donahue R, Wade C, Storm DR (1998) Stimulation of cAMP response element (CRE)-mediated transcription during contextual learning. Nat Neurosci 1:595–601.

Irvine EE, Vernon J, Giese KP (2005) αCaMKII autophosphorylation contributes to rapid learning but is not necessary for memory. Nat Neurosci 8:411–412.

Izquierdo I, Bevilaqua LR, Rossato JI, Bonini JS, Medina JH, Cammarota M (2006) Different molecular cascades in different sites of the brain control memory consolidation. Trends Neurosci 29:496–505.

Lisman J, Schulman H, Cline H (2002) The molecular basis of CaMKII function in synaptic and behavioural memory. Nat Rev Neurosci 3:175–190.

Lorenzini CA, Baldi E, Bucherelli C, Sacchetti B, Tassoni G (1996) Role of dorsal hippocampus in acquisition, consolidation and retrieval of rat's passive avoidance response: a tetrodotoxin functional inactivation study. Brain Res 730:32–39.

Malenka RC, Bear MF (2004) LTP and LTD: an embarrassment of riches. Neuron 44:5–21.

Matsuzaki M, Honkura N, Ellis-Davies GC, Kasai H (2004) Structural basis of long-term potentiation in single dendritic spines. Nature 429:761–766.

Mukherji S, Soderling TR (1994) Regulation of Ca^{2+}/calmodulin-dependent protein kinase II by inter- and intrasubunit-catalyzed autophosphorylations. J Biol Chem 269:13744–13747.

Nishioka N, Shiojiri M, Kadota S, Morinaga H, Kuwahara J, Arakawa T, Yamamoto S, Yamauchi T (1996) Gene of rat Ca^{2+}/calmodulin-dependent protein kinase IIα isoform—its cloning and whole structure. FEBS Lett 396:333–336.

Okabe S, Kim HD, Miwa A, Kuriu T, Okado H (1999) Continual remodeling of postsynaptic density and its regulation by synaptic activity. Nat Neurosci 2:804–811.

Okabe S, Urushido T, Konno D, Okado H, Sobue K (2001) Rapid redistribution of the postsynaptic density protein PSD-Zip45 (Homer 1c) and its differential regulation by NMDA receptors and calcium channels. J Neurosci 21:9561–9571.

Okamoto K, Nagai T, Miyawaki A, Hayashi Y (2004) Rapid and persistent modulation of actin dynamics regulates postsynaptic reorganization underlying bidirectional plasticity. Nat Neurosci 7:1104–1112.

Okamoto K, Narayanan R, Lee SH, Murata K, Hayashi Y (2007) The role of CaMKII as an F-actin-bundling protein crucial for maintenance of dendritic spine structure. Proc Natl Acad Sci U S A 104:6418–6423.

Otmakhov N, Tao-Cheng JH, Carpenter S, Asrican B, Dosemeci A, Reese TS, Lisman J (2004) Persistent accumulation of calcium/calmodulin-dependent protein kinase II in dendritic spines after induction of NMDA receptor-dependent chemical long-term potentiation. J Neurosci 24:9324–9331.

Sakagami H, Matsuya S, Nishimura H, Suzuki R, Kondo H (2004) Somatodendritic localization of the mRNA for EFA6A, a guanine nucleotide exchange protein for ARF6, in rat hippocampus and its involvement in dendritic formation. Eur J Neurosci 19:863–870.

Shen K, Meyer T (1999) Dynamic control of CaMKII translocation and localization in hippocampal neurons by NMDA receptor stimulation. Science 284:162–166.

Shen K, Teruel MN, Connor JH, Shenolikar S, Meyer T (2000) Molecular memory by reversible translocation of calcium/calmodulin-dependent protein kinase II. Nat Neurosci 3:881–886.

Silva AJ, Stevens CF, Tonegawa S, Wang Y (1992) Deficient hippocampal long-term potentiation in α-calcium-calmodulin kinase II mutant mice. Science 257:201–206.

Stoppini L, Buchs PA, Muller D (1991) A simple method for organotypic cultures of nervous tissue. J Neurosci Methods 37:173–182.

Taniguchi M, Sanbo M, Watanabe S, Naruse I, Mishina M, Yagi T (1998) Efficient production of Cre-mediated site-directed recombinants through the utilization of the puromycin resistance gene, pac: a transient gene-integration marker for ES cells. Nucleic Acids Res 26:679–680.

Taylor SS, Buechler JA, Yonemoto W (1990) cAMP-dependent protein kinase: framework for a diverse family of regulatory enzymes. Annu Rev Biochem 59:971–1005.

Tomita S, Stein V, Stocker TJ, Nicoll RA, Bredt DS (2005) Bidirectional synaptic plasticity regulated by phosphorylation of stargazin-like TARPs. Neuron 45:269–277.

Whitlock JR, Heynen AJ, Shuler MG, Bear MF (2006) Learning induces long-term potentiation in the hippocampus. Science 313:1093–1097.

Yagi T, Aizawa S, Tokunaga T, Shigetani Y, Takeda N, Ikawa Y (1993) A role for Fyn tyrosine kinase in the suckling behaviour of neonatal mice. Nature 366:742–745.

Yamagata Y, Imoto K, Obata K (2006) A mechanism for the inactivation of Ca^{2+}/calmodulin-dependent protein kinase II during prolonged seizure activity and its consequence after the recovery from seizure activity in rats in vivo. Neuroscience 140:981–992.

Yamauchi T, Ohsako S, Deguchi T (1989) Expression and characterization of calmodulin-dependent protein kinase II from cloned cDNAs in Chinese hamster ovary cells. J Biol Chem 264:19108–19116.

Yanagawa Y, Kobayashi T, Ohnishi M, Kobayashi T, Tamura S, Tsuzuki T, Sanbo M, Yagi T, Tashiro F, Miyazaki J (1999) Enrichment and efficient screening of ES cells containing a targeted mutation: the use of DT-A gene with the polyadenylation signal as a negative selection maker. Transgenic Res 8:215–221.

Zhang YP, Holbro N, Oertner TG (2008) Optical induction of plasticity at single synapses reveals input-specific accumulation of αCaMKII. Proc Natl Acad Sci U S A 105:12039–12044.